Article

Application of multi-scale mathematical model in optimization of cellular metabolic network

Hongtao Wang[*], **Yulei Wang**

Department of Basic Courses, Xinxiang Vocational and Technical College, Xinxiang 453006, China
* Corresponding author: Hongtao Wang, htwang361@126.com

Abstract: A cellular metabolic network is an intricate system of biochemical routes and reactions that allow a cell to grow, survive, and operate. These networks handle the conversion of nutrients into energy, building blocks for cell structures, and other bioactive compounds required for cellular functions. The metabolic network's complex physiological function in completing the catalytic conversion could be completely comprehended from a whole-body viewpoint, which considers the underlying interactions between the metabolic conditions of the body as a whole, surrounding tissue, and specific cells. Research presents a multi-scale mathematical model to optimize cellular metabolic networks by integrating cellular-level metabolic processes with whole-body physiological systems. This approach integrates dynamic flux balance analysis with refined genetic algorithms (RGA) to optimize enzyme activities and metabolic fluxes. The liver material of a physiologically based adult pharmacokinetic (PB-PK) classical was used to evaluate the methods using a genome-scale network rebuilding of a humanoid hepatocyte. A systems-level investigation of hyper uricemia treatment, liver metabolism, detoxification pathway simulation, and PB-PK models was conducted using the multi-scale model that was produced. This model offers a framework for metabolic optimization, facilitating an improved understanding of medication discovery and illness treatment approaches.

Keywords: multi-scale; cellular metabolic network; refined genetic algorithm (rga); physiologically-pharmacokinetic (PB-PK); genome-scale

1. Introduction

In the past few years, genome sequencing skills have advanced significantly, with the quantity of genome sequences has grown dramatically. Increasing volumes of genetic statistics have been made available, allowing investigators to explore the metabolic mechanisms of bacteria in greater complexity and significantly endorsing the growth of connected fields [1]. By using these massive amounts of data to investigate the mechanisms of life behavior comprehensively it is a significant issue [2]. The biological system is extremely complicated, requiring various molecules with specific characteristics to keep up normal biological functioning via nonlinear interactions with one another [3]. Computers are capable of carrying this task through simulation, allowing researchers to better comprehend the difficult architecture of live schemes. To address this demand, genome-scale metabolic network models (GEMs) were developed. GEMs use a series of appropriately stable biological responses to generate a mathematical matrix that forecasts the target organism's metabolic phenotype [4]. Because industrial microbes' intracellular metabolic processes are extremely complicated, investigators have created urbane and complicated metabolic networks during their history. Metabolic simulations have been used to optimize strain

design for improved try of bioproducts. GEMs, which include precise gene-protein-reaction connections (GPRs), are commonly employed for studying strain metabolism. Metabolic models can predict genes focused on high productivity in industrial chassis strains and provide a framework for analyzing omics data [5]. This can indicate the process underlying a specific phenotype, such as high product productivity. GEMs have been created for over 6239 organisms using human or automated processes. Flux balance analysis (FBA) is an extensively used technique to describe cellular metabolism, with dynamic FBA procedures [6]. However, FBA has restrictions due to assumptions on steady-state with substrate approval rates. To enhance the application scope of GEMs, classical examination algorithms constructed on multi-omics data have been urbanized [7]. To create multi-scale GEMs, a variety of genomics databases and model-building methods have been established. Massive omics data have driven the interpretation of biological systems as high-throughput technologies have advanced [8]. Machine learning (ML) has developed a must-have technique for training and analyzing huge datasets, resulting in a plethora of ML-trained GEMs that incorporate multilevel omics data to provide deeper insights into genotype-phenotype interactions. The single gene-protein-reaction link in Generalized Error Modeling can lead to errors due to the multi-dimensional, rule of microbial metabolism [9]. Multi-scale GEMs, which include restrictions or incorporate omics data, evolved from conventional GEMs and are frequently utilized in silicon bio-design. It looks at the construction workflow & toolkits for multi-scale models, whether artificial intelligence (AI) could enhance their quality, and future difficulties and opportunities in multi-scale GEM development. It could help biological engineers construct adaptable factories of cells for sustainable bioproduction. The research presents a multi-scale mathematical framework that connects cellular metabolism to whole-body physiological systems, allowing for greater comprehension and optimization of these processes [10]. Research goal is to create and deploy a multi-scale mathematical model for optimizing cellular metabolic networks. The concept aims to increase awareness of complex biochemical pathways and control over these processes by connecting cellular processes to whole-body systems. This optimization seeks to promote advances in drug research, disease therapy (such as managing excessive uric acid levels), and liver function analysis, resulting in a more effective framework for studying and applying cellular metabolism in real-world healthcare settings.

Key contributions of the research

- Development of a multi-scale mathematical model for optimization of cellular metabolic networks.
- Implementation of dynamic flux balance and improved genetic algorithms for metabolic optimization
- Simulation of the metabolic and detoxification pathways due to the therapeutic and toxic paracetamol doses.
- Analysis and comparison of different treatment strategies for hyperuricemia, like allopurinol, specific enzyme inhibition, and lifestyle adjustments, along with their respective impacts on metabolic health.

- Proof of the concept about the efficacy of the model in optimizing treatment outcomes for metabolic health.

The paper follows a relatively systematic flow of work, with Phase 1 introducing the issue, Phase 2 examining relevant work, Phase 3 mentioning the methodology, Phase 4 presenting results, Phase 5 covering the discussion and limits, and Phase 6 concluding with major conclusions and future direction. This structured framework ensures that the flow of thought remains clear and logical throughout the text.

2. Related work

The growing demand for microbial-produced goods needs optimal designs for microbiological cell factories via metabolic engineering. ML and intellectual optimization-based methods have gained popularity in GEMs that employ limited optimization methods [11]. The work examines the evolution of GEMs, introduces constraint-based analysis approaches, and discusses the use of ML and intelligent optimization procedures in GEM prototypes. It also addresses research gaps and future study opportunities in ML and intellectual optimization approaches that are functional in GEMs.

Cellular regulation and metabolic engineering depend on GEMs [12]. Their reliance on a single gene-protein-reaction data format restricts understanding of biological complexity. Multi-scale models, such as multi-constraint, multi-omic, and whole-cell models, have been created to reliably predict phenotype from genotype. The article examined recent achievements in multi-scale GEM development, including frameworks, toolkits, and algorithms, as well as difficulties and viewpoints.

Cancer cells use anaerobic metabolic pathways and use more glucose than healthy cells, regardless of metabolic differences [13]. These biological concerns are addressed using laboratory and mathematical representations; the paper investigated the ability of computational modeling to uncover the function of reprogramming the metabolism in tumor progression.

The biotechnology sector was a diverse subject that prioritized digitization and the improvement of numerous aspects. Cutting-edge modeling concepts are categorized and their uses, advantages, and disadvantages are examined in the work [14]. The paper proposes employing scale-down principles & analytical instruments to capture the intracellular conditions of individual cells. The goal is to create computer models that are appropriate for the cell design of plants and process optimization on an industrial scale.

Artificial intelligence (AI) and synthetic biology advancements have opened up new possibilities for contemporary biotechnology, particularly the high-performance manufacturing of cells proposed by the article [15]. White-box approaches and AI-powered stress engineering have been established, but each has benefits and drawbacks. Deep integration of AI and metabolic models is required for better cell manufacturing with greater yields and higher production rates.

For the rapid design and deployment of great presentation microbial cell factories (MCFs), the development of 16 essential industrial GEMs was examined in [16] publication. In silico, the models could replicate the metabolic parameter mechanism of microorganisms, providing useful support for the quick creation of MCFs. Research

discussed the use of GEMs to guide metabolic engineering, such as examining and explaining metabolic aspects, forecasting the impacts of genetic alterations on metabolism, forecasting ideal phenotypes, and leading cell factory creation in actual studies.

Over the past 20 years, thousands of GEMs have been constructed, with uses ranging from cell phenotypic prediction to network interaction presented in work [17]. However, because research had no restrictions, first-generation GEMs had poor prediction accuracy. Next-generation GEMs combine omics data, constraint conditions, physiological models, and whole-cell simulations. Research were employed in the industrial field of biotechnology, human health, and research into biological systems. Challenges and emerging developments in GEMs are addressed.

Recent flux simulation methods for microbial systems are the main topic of the author [18]. The pseudo-steady hypothesis can be used to quickly mimic stable metabolic states in single-microbial systems, which are straightforward. These systems are more accessible than multifaceted systems, which can reduce metabolic stress by division, resource trading, and sophisticated substrate co-utilization, but few studies have focused on simulation techniques for polymicrobial metabolic flux.

The Valley of Death is having trouble commercializing biotechnology for industrial usage, according to the reference [19], which associates automation, AI, and computation. Intelligent bio manufacturing consists of three steps: digitalization, demonstrating, and intellectualization, serving as a critical connection. The work examined mechanistic and data-driven models, mixed models, stress design, control of processes, optimization, and bioreactor scale-up, as well as the difficulties and potential for biomanufacturing in the context of Industry 4.0.

Applications in biotechnology may arise from synthetic microbial communities, which blend various strains for the best interactions and nutrition. Due to their ability to precisely predict organism features and explore molecular processes, GEMs are helpful tools for foretelling and constructing these communities [20]. Despite their youth, GEM-based techniques were increasingly being employed to create synthetic microbial communities, lowering trial-and-error costs and increasing functionality.

Progress in comprehending and creating microbial communities with different GEMs is covered in the current work [21]. It highlights how the subject was evolving from single-strain to bacterial community level, presents a framework for creating GEMs, and investigates the role that intracellular and external resources play in community development. It also highlights GEM's limitations and potential objectives, such as connection with quorum sensing methods and machine learning techniques.

Although it usually lacks dynamic interactions and cell-specific characterization, agent-based modeling might be useful in biological articles [22]. Real-size, scalable models of biological systems were necessary to capture both system-wide emergent traits and cell-to-cell heterogeneity. These simulations were delivered via high-performance computing clusters, making them more similar to digital twins.

Constraint-based modeling (CBM) is a fundamental system biology method that depicts the link between genotype, phenotype, and surroundings. High-throughput experimental techniques and multi-omics approaches have yielded fresh insights from a variety of biological fields that were examined in the reference [23]. Integrating these

techniques could enhance bioengineering and applications in medicine, hence, increasing the use of ML-based CBM for both society and the environment.

A mixture of mathematical models of growth & response to different chemotherapy treatments was developed by the author [24]. The model simulated the growth of a tumor in three dimensions and examined how it reacts to different chemotherapy methods. The outcomes demonstrated that conjoining anti-angiogenic drugs with anti-cancer medications increases therapeutic efficacy while reducing negative effects. The model also identifies tumor form and cell phenotypic distribution as distinguishing features between treatment approaches.

The complex process of industrial biosynthesis is controlled by chemicals, genes, and fermenter design. It is challenging to identify species to raise reaction titers. Recent developments in biosynthesis titer increase were described by the work [25], with an emphasis on data-driven process optimization and metabolic pathway retraining. More quantitative information can be obtained by combining multi-scale data with mathematical replicas.

Problem statement of the research: Metabolic Network Optimization is a need for a model that integrates cellular metabolic processes with whole-body physiological systems to improve metabolic functions and treatment effects. Paracetamol Dose Effects in several paracetamol dosages on metabolic and detoxifying pathways must be better explored using simulation-based studies. In personalized medicine existing metabolic models do not adequately account for unique patient profiles, emphasizing the necessity for personalized simulations to optimize treatment regimens.

3. Materials and methods

Research utilized the form of optimization of cellular metabolic networks that utilize multi-scale PB-PK modeling, dynamic flux balance analysis, and improved genetic algorithms towards an integrated cellular and whole-body physiology approach in drug discovery and the treatment of disease.

3.1. Multi-scale PB-PK modeling for integrating cellular metabolism and whole-body physiology

The PB-PK modeling, multi-scale modeling at the whole-body level is useful for developing a quantitative framework to understand all the spreading, absorption, and excretion processes of both natural processes and extrinsic mixes in mammalian bacteria. As compared with traditional compartmental models, which usually involve a general view of pharmacokinetics, multi-scale models feature explicit representations of physiological processes driven by the latest knowledge and data. Such a model links sub-compartments in different tissues and sub-compartments of the vascular system, applying distribution models to quantify mass transfer across sub-compartments.

The distribution parameters are determined from the physicochemical properties of compounds, such as molecular weight and lipophilicity. Physiological parameters, including tissue capacities, blood flow rates, and flesh configuration, are cleaned from well-curated biological datasets. Such a comprehensive model structure is supported by large prior data collections; the compound-specific parameters necessitate minor

modifications, whereas physiological parameters are handmade for an organism. This differentiation ensures the robustness of the framework, combining systemic and cellular levels and cell metabolism that is optimized and ready for applications in drug discovery and treatment of diseases.

The dataset contains a large amount of parameters of individual physiology, mainly including age, weight and height and so on, which is very closer to establish a precise multi-scale PB-PK model. This data enables highly accurate constructions of tissue compartments and metabolism action plans at the cellular and whole body frame works. These individual-specific variables that have been incorporated into the model allow for representation of the differences in metabolic rates across individuals which in return improves on the model's performance. This dataset is then used to parameterize and optimize the model using software from PK-Sim and MoBi which allows the integration and verification of key cellular metabolic networks in different whole body biochemical systems. These tools are involved in the establishment of metabolic pathways and the elective variation of kinetic constants to address the model's flexibility according to cellular and systemic variations. This makes the dataset very valuable for optimizing metabolic networks as well as evaluating and designing drug discovery and treatment of different metabolic diseases.

Stoichiometric network models: Stoichiometric models impose a framework of mathematical structure upon the inherent biochemistry of cellular metabolism to capture an analytical framework. Assuming that each cellular metabolite is in a steady state, such models allow the balancing of all intracellular metabolites with linear equations, although the system has more unfamiliar response charges than independent mass equilibrium equations. It uses flux balance analysis to leverage stoichiometric models to analyze optimal flux distributions over the metabolic network. This could allow evaluating and optimizing some key metabolic pathways efficiently to help meet the goal of improving cellular metabolic network efficacy and functionality:

$$\min/\max e.u$$

$$\text{s.}\,t.\,T.\,u = 0$$

$$\text{A.}\,u \leq a$$

$$u_{min} \leq u \leq u_{max} \tag{1}$$

where $e.u$ is the objective function describing a focused aspect of cellular performance that needs to be maximized. Here u is the distribution of flux inside the cell over all these n reactions. The solution space for this system is also restricted by other considerations $A.u \leq a$, which include details of substrate availability as well as other physiological constraints. These constraints will ensure realism in the adherence of the model to the metabolic conditions of the cell, and therefore, optimization toward network efficiency is achievable with precise accuracy.

HepatoNet1: By utilizing HepatoNet1, a liver-specific metabolic network model, to optimize cellular metabolic networks at the tissue level. This model comprises 780 metabolites and 2550 reactions, organized in seven intracellular and three extracellular compartments. Validated through 125 biochemical objectives representing feasible metabolic functions, HepatoNet1 offers a reliable framework to explore distinct

metabolic processes in liver tissue. By incorporating this network, it aims to analyze and optimize liver-specific metabolic pathways, supporting the objective of integrating cellular-level processes with whole-body systems for enhanced insights into drug efficacy and disease treatment strategies.

3.2. Dynamic flux balance analysis (DFBA)

3.2.1. Intracellular flux balance model

For applying DFBA to optimize cellular metabolic networks in the research, it is essential to develop a detailed metabolic network model for each target species. Typically, GEM reforms are recycled because model offer strong predictive capabilities and map gene-protein-reaction relationships accurately. This approach is effective given the growing database of genome-scale models, especially for well-characterized species. Traditionally, manual curation was required for building these metabolic models. However, computational tools like Model SEED, Pathway Tools, and Microbes Flux allow automated generation of draft models, saving time. Given the availability of the required genome-scale reconstructions, each species' stoichiometric model in Equation (2).

$$B_j u_j = 0 \ u_{j,min} \leq u \leq u_{j,max} \tag{2}$$

The B_j is represented as a stoichiometric matrix and the flux vector of each cell's reaction is u_j. The flux bounds, such that $u_{j,min}$, and $u_{j,max}$ give the j_{th} species. By integrating all these matrices and their constraints towards all the m species, create a composite stoichiometric network model. Then, this unified model helps in simulating and optimizing metabolic interactions across various species in the cellular network.

$$\begin{bmatrix} B_1 & 0 & 0 & 0 \\ 0 & B_2 & 0 & 0 \\ 0 & 0 & \ddots & 0 \\ 0 & 0 & 0 & B_m \end{bmatrix} \begin{bmatrix} u_1 \\ u_2 \\ \vdots \\ u_m \end{bmatrix} = \begin{bmatrix} 0 \\ 0 \\ \vdots \\ 0 \end{bmatrix} \Rightarrow Bu = 0$$

$$\begin{bmatrix} u_{1,min} \\ u_{2,min} \\ \vdots \\ u_{m,min} \end{bmatrix} \leq \begin{bmatrix} u_1 \\ u_2 \\ \vdots \\ u_m \end{bmatrix} \leq \begin{bmatrix} u_{1,max} \\ u_{2,max} \\ \vdots \\ u_{m,max} \end{bmatrix} \Longrightarrow u_{min} \leq u \leq u_{max} \tag{3}$$

DFBA splits each species inside the metabolic network into a single compartment, while metabolites exchange in a time-varying way through an extracellular compartment, outperforming classical. The FBA technique assumes constant metabolite exchange rates. This model combines interspecies compartments as organelles, interspecies compartments without metabolite exchange, and an extracellular compartment. This optimizes fluxes by maximizing substrate absorption fluxes for the community. Assuming that the overarching purpose of the communal is to optimize its entire growth rate, the OptCom framework allows for both species-specific and community-level optimal performance. This premise offers a following Linear Program (LP) issue with a multispecies allowance in Equation (3).

$$\max_{u} \mu = \mu_1 + \mu_1 + \cdots + \mu_m = x^S u \tag{4}$$

$$Bu = 0$$

$$u_{min} \leq u \leq u_{max}$$

Equation (4) defines the stoichiometric matrix B, as well as the flux vectors u, u_{min}, and u_{max}, and x is a partition trajectory of feedstock evaluating coefficients. Classical FBA applies to a community model by describing individual species' substrate uptake fluxes and accounting for unidentified fluxes. Species relations could be simulated using metabolite conversation, pretentious that the overall generation amount of each free metabolite equals the entire absorption rate of other species. The DFBA technique permits released metabolites to build up &influence absorption rates, presenting limits on species interactions.

3.2.2. Extracellular dynamic model

The extracellular dynamic model and the assumptions outlined above are unique to the traditional FBA challenge. It assumes that the rate of metabolite exchange between community members is constant. It assumes that this metabolite must be eaten in proportion to its production, which allows us to loosen the approach to DFBA. The growth rates, intracellular fluxes, and product release fluxes of each species in the community are calculated. The model includes dynamic extracellular mass balances for expended substrates and concealed goods, which are numerically integrated to calculate biomass, substrate, and product concentrations as a function of time. Fluxes for species that do not consume a specific substrate or produce a specific product are assigned 0 values. Additionally, the model now includes mass balances for gas substrates, including oxygen levels. These variables can be determined empirically and used to evaluate the modeling construct. Outside of the cell, substrate focus & production levels are employed to manage time-dependent.

DFBA is a method used to research the uptake kinetics of substrates and species. It uses expressions for uptake kinetics, which represent the maximum rates possible due to transport limitations. The main challenge is identifying the suitable uptake kinetics among all substrate or species couples. If a species is recognized to consume a substrate, the component u_{tj} connected with that substrate could be agreed to zero. DFBA offers an advantage over classical FBA by allowing complex regulatory mechanisms like diauxic substrate consumption and growing reserve by extracellular metabolites to be involved in a phenomenological method. Commonly used approval expressions are included in Equation (5).

$$u_{tj} = \frac{u_n T_i}{L_n + T_i}$$

$$u_{tj} = \frac{u_n T_i}{L_n + T_i} \frac{1}{1 + T_l/L_t}$$

$$u_{tj} = \frac{u_n T_i}{L_n + T_i} \frac{1}{I + O_l/L_o} \tag{5}$$

where T_i and T_l are the absorption of substrates i & l, separately, O_l is the absorption of product L, u_n and L_n are the Michaelis Menten constants, L_t & L_o are the reserve coefficients. Equation (5) covers merely substrate-limited approval, while the

subsequent equation includes absorption restriction by a favored substrate; Equation (3) captures the species interactions wherein one of the species' metabolic by-products prevents the uptake rate of another species' substrate. Such a system can be obtained by combining prior knowledge with iterative modeling to derive its dynamic solution. The sequential approach is computationally incompetent and prone to constancy difficulties, though easy to conceptualize. In contrast, the simultaneous approach integrates the approval kinetics and the LP directly into the extracellular equations for a more effective solution. This approach of a differential-algebraic calculation scheme is more reliable and computationally efficient, since it solves the embedded LP only when significant changes occur in the optimal flux distribution, thereby taking fewer LP solutions than integration steps are displayed in **Figure 1**.
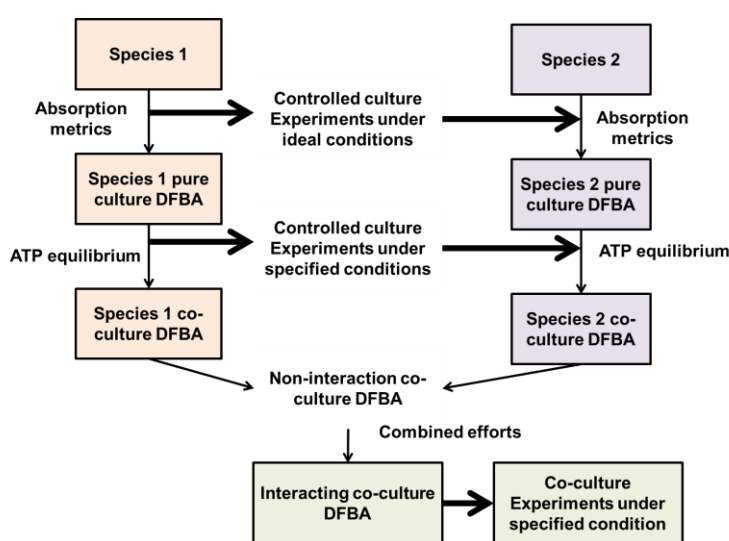
Figure 1. Framework of dynamic flux balance analysis.

This approach uses genome-scale metabolic reconstructions to create a stoichiometric matrix for each species, which is combined into a multi-species network optimized for community-level objectives like maximizing growth. By including difficult controlling devices, such as diauxic changes and inhibition by extracellular by-products, DFBA captures interspecies interactions and trade-offs that influence metabolic efficiency. To solve the non-linear system of differential equations embedded with linear programming, DFBA applies efficient numerical methods, with differential-algebraic equations offering computational stability. Ultimately, DFBA provides a powerful framework for optimizing metabolic interactions in cellular communities, with applications in biotechnological engineering, microbial community design, and synthetic biology.

3.3. Refined genetic algorithm (RGA)

RGA are strong search techniques used in our process. A simple GA workflow involves the generation of an initial population comprising candidate solutions, which are then referred to as chromosomes. The solutions are then assessed using a fitness function. Chromosomes are then designated for genetic operations such as crossover & mutation. Offspring created from these operations switch their parents in the population. This cycle recaps itself until a predefined stopping condition is met.

Research modified the traditional GA approach by introducing new genetic operators to enhance its performance, as illustrated in our improved GA process. The detailed steps of this modified GA will be described in the following sections.

Initial Population: The beginning population represents a possible clarification fixed at O. Typically, the initial population is produced at random.

$$O = \{o_1, o_2, \ldots, o_{pop_{size}}\} \tag{6}$$

$$O_j = \begin{bmatrix} o_{j_1} & o_{j_2} & \cdots & o_{j_i} & \cdots & o_{j_{no\_vars}} \end{bmatrix}, j = 1,2,\ldots,pop_{size}; i = 1,2,\ldots,no\_vars \tag{7}$$

$$para_{min}^i \leq o_{j_i} \leq para_{max}^i \tag{8}$$

pop_{size} Represents the total number of candidate solutions (population size). The no_{vars} indicate the number of variables to be optimized. For each solution $j = 1,2,\ldots,pop_{size}; i = 1,2,\ldots,no\_vars$ are the parameters that need to be tuned. The values $para_{min}^i$ and $para_{max}^i$ represent the minimum and maximum allowable values for each parameter o_{j_i} across all solutions. This structure results in a set of potential solutions, where each solution o_j is a chromosome consisting of the tunable variables o_{j_i}.

Evaluation: For every chromosome in the population, an appropriate fitness function will be computed. The fitness function computes a measure of quality for each solution, with better quality of the solutions having higher fitness values. This will identify the best solutions for the problem under consideration. The fitness function used in the evaluation of a chromosome in the population is described in the below Equation (9).

$$fitness = e(o_j) \tag{9}$$

The application determines the structure of the fitness function.

Selection: a roulette wheel selection method where two candidate solutions selected from the population are operated for reproduction. This method ensures the probability of selection of chromosomes with higher fitness values is higher, adhering to the fact that a better solution has more chances of producing better offspring. The process of selection involves assigning each chromosome a selection probability r_j, with o_i assigned to everyone with a given probability, in this case where higher fitness values indicate a greater chance of being selected.

$$r_j = \frac{e(o_j)}{\sum_{i=1}^{pop\_size} e(o_i)}, j = 1,2,\ldots,pop\_size \tag{10}$$

The cumulative probability $\hat{r}_j$ for the chromosome o_i is in Equation (11),

$$\hat{r}_j = \sum_{i=1}^{j} r_i, j = 1,2,\ldots,pop\_size \tag{11}$$

In the selection procedure, it started by arbitrarily producing a nonzero floating-point numeral $x \in [0\ 1]$. A chromosome is selected if the condition $r_{j_{-1}}$ holds, where $\hat{r}_j = 0$. This ensures that chromosomes with higher fitness values $e(o_j)$ have a higher

probability of being selected. As a result, the finest chromosomes will generate extra offspring, while the normal & poorest performing chromosomes will either stay or be removed. Only dual chromosomes are selected to undertake the genetic processes in this step.

Genetic Operations: It generates fresh offspring chromosomes from the chosen parents resulting from the selection procedure. The two main techniques implicated in these operations are crossover and mutation.

3.4. Crossover

This operation of crossover is a kind of interaction between two solutions, which are intended to be exchanged. These solutions are derived from the population. In this way, two parents will give rise to one offspring. Here are the details of the crossover operation: Four candidate solutions will be produced based on the following Equations (12–17).

$$pt_d^1 = [pt_1^1 \quad pt_2^1 \quad \cdots \quad pt_{no\_vars}^1] = \frac{O_1 + O_2}{2} \tag{12}$$

$$pt_d^2 = [pt_1^2 \quad pt_2^2 \quad \cdots \quad pt_{no\_vars}^2] = O_{max}(1-x) + \max(o_1, o_2)x \tag{13}$$

$$pt_d^1 = [pt_1^3 \quad pt_2^3 \quad \cdots \quad pt_{no\_vars}^3] = O_{min}(1-x) + \max(o_1, o_2)x \tag{14}$$

$$pt_d^1 = [pt_1^4 \quad pt_2^4 \quad \cdots \quad pt_{no\_vars}^4] = \frac{(O_{max}+)(1-x) + \max(o_1, o_2)x}{2} \tag{15}$$

$$o_{max} = [para_{max}^1 \quad para_{max}^2 \quad \cdots \quad para_{max}^{no\_vars}] \tag{16}$$

$$o_{min} = [para_{min}^1 \quad para_{min}^2 \quad \cdots \quad para_{min}^{no\_vars}] \tag{17}$$

where $x \in [0\ 1]$ represents the mass to be resolute by users, $\max(o_1 o_2)$ indicates the trajectory with each component gained by consuming the maximum corresponding component of o_1 and o_2. For instance, $\min([1 \quad -2 \quad 3], [2 \quad 3 \quad 1]) = [2 \quad 3 \quad 3]$. Between pt_d^1 to pt_d^3, the one with the highest fitness cost is utilized as the offspring of the crossover operation. The offspring is in Equation (18).

$$pt = [pt_1 \quad pt_2 \quad \cdots \quad pt_{no\_vars}] = pt_c^{ios} \tag{18}$$

The crossover procedure generates offspring with the highest value of ios, where $e(pt_d^j), j = 1,2,3,4$. If the crossover process produces good offspring, an advanced fitness cost can be achieved in less repetition. The offspring spread over the domain, moving near the center region and near the domain boundary. The offspring's fitness value can be achieved in fewer iterations if the crossover operation produces an offspring.

3.5. Mutation

The offspring of Equation (18) will go through the mutation surgery. Mutations alter the genes on chromosomes. As a result, inherited chromosomal traits can change. The mutation process generates three new offspring in Equation (19).

$$nos_i = [pt_1 \quad pt_2 \quad \cdots \quad pt_{no\_vars}] + [a_1 \Delta nos_1 \quad a_2 \Delta nos_2 \quad \cdots \quad a_{no\_vars} \Delta nos_{no\_vars}], i = 1,2,3 \qquad (19)$$

where $a_j, j = 1,2,..,no\_vars$ and $\Delta nos_j, j = 1,2,...,no\_vars$ the text describes a method for generating new offspring using a random number generator. The first offspring ($i = 1$) is generated with one randomly chosen a_j as the maximum, the second offspring with some a_j as the minimum, and the third offspring with all a_j as the maximum. These offspring are assessed using the fitness purpose of Equation (4), which generates a real number and compares it with a user-defined amount o_b. If the actual amount is more than the initial offspring drive inherit the chromosome by the lowest fitness cost sf in the population. The possibility of adopting a substandard offspring is used to limit the likelihood of convergence to a native optimal, maintaining the potential of attaining the worldwide optimal. This broader search space allows for a flexible exploration of potential solutions. After selection, crossover, and mutation, an original population is shaped and the procedure iterates till a predefined end. The improved genetic algorithm (IGA) refines the solution space toward an optimal configuration for optimizing species-specific parameters in metabolic network models.

4. Result

The results indicate that therapeutic amounts of therapy lower uric acid levels while enhancing liver detoxification & metabolic processes, but toxic doses cause considerable damage. The multi-scale approach gives insights into metabolic network optimization, as well as a foundation for designing efficient hyperuricemia management techniques & improving overall metabolic health.

Table 1. Hyperuricemia treatment simulation table.

Treatment	Time Point	Uric Acid Concentration (mg/dL)	Liver Detoxification (%)	Metabolic Function Improvement (%)
Baseline	-	7.0 -Initial level	100 Baseline	0 Baseline
Therapeutic	Mid-point	5.5 - Reduced	115 - Moderate improvement	15
Therapeutic	End-point	4.0 - Target level	125- High improvement	25
Toxic	Mid-point	8.5 - Elevate	90 - Moderate reduction	−10
Toxic	End-point	10.0 - Very high	75 - Severe impairment	−25

Table 1 depicts the properties of several actions on the concentration of uric acid, liver detoxification, and improvement of metabolic function at different time points. At baseline, uric acid levels are high at 7.0 mg/dL, with liver detoxification and metabolic function at the base level; that is, at 100% and 0%, respectively. At the end of treatment, uric acid levels decrease to 5.5 mg/dL and 4.0 mg/dL, and detoxification and metabolism functions in the liver are improved to 115% and 125%, with the reflection of a positive impact of treatment. Conversely, in the toxic phase, uric acid dramatically increases to 8.5 mg/dL and 10.0 mg/dL, wherein liver detoxification and metabolic function weaken to 90% and 75%, respectively, in the end, showing the adverse effects of overmedication. This information contributes to the purpose of optimizing cellular metabolic networks with a multi-scale mathematical model, which covers the cellular metabolic process and whole-body physiological systems; such

results will help develop predictive and optimizing treatment strategies for hyperuricemia, improve the level of detoxification by the liver, and enhance overall metabolic functions without causing harmful toxic effects.

Table 2 describes the modulation of paracetamol treatment on fluxes of various metabolic pathways at therapeutic and toxic doses. At the therapeutic dose, glucose, amino acid, fatty acid, and detoxification pathway flux values are highly noticed, with end-point values reaching 98%, 99%, 98%, and 99%, respectively, to indicate normal metabolic function. However, at a toxic dose of 15 g, fluxes have significantly come down and only glucose, amino acid, fatty acid, and detoxification pathway fluxes reached 25%, 30%, 20%, and 40% of their original values, respectively, at the end-point, showing an impaired metabolism and detoxification. The 6g–10g (Therapeutic) dose shows moderate improvements in metabolic fluxes: at mid-point, glucose (85%), amino acid (92%), fatty acid (80%), and detoxification (90%). By the end-point, values improve to glucose (88%), amino acid (94%), fatty acid (85%), and detoxification (92%). This data validates the purpose of the multi-scale model, which makes the metabolic network optimal by showing the effect of toxic doses on the metabolic and detoxification pathways, an understanding of how essential it is to understand drug-induced metabolic alterations.

Table 2. Impact of paracetamol doses on metabolism at different time points.

Paracetamol Treatment Regimen	Time Point	Glucose Metabolism Flux (%)	Amino Acid Metabolism Flux (%)	Fatty Acid Metabolism Flux (%)	Detoxification Pathway Flux (%)
1 g–5g(Therapeutic)	Mid-point	95	98	90	97
	End-point	98	99	98	99
6g–10g (Therapeutic)	Mid-point	85	92	80	90
	End-point	88	94	85	92
11g–15g (Toxic)	Mid-point	40	50	30	60
	End-point	25	30	20	40

Table 3 indicates the effects of different treatment strategies on uric acid reduction, enzyme activity change, metabolic flux change, and success rate. For Allopurinol (Drug X), uric acid is reduced by 3.5 mg/dL, with a 20% decrease in enzyme activity and a 10% reduction in metabolic flux, achieving an 85% success rate. Enzyme inhibition (Xanthine Oxidase) leads to a greater reduction in uric acid (4.2 mg/dL), with a 30% decrease in enzyme activity and a 12% reduction in metabolic flux, yielding a 90% success rate. Lifestyle changes (diet/exercise) reduce uric acid by 2.0 mg/dL, with a 10% decrease in enzyme activity and a 5% reduction in metabolic flux, showing a 70% success rate. This data supports the objective of optimizing cellular metabolic networks through the multi-scale model, which can simulate and compare the effects of these treatments on enzyme activity and metabolic flux to identify the most effective strategies for reducing uric acid and improving overall metabolic health.

Table 3. Treatment efficacy table.

Treatment Strategy	Uric Acid Reduction (mg/dL)	Enzyme Activity Change (%)	Metabolic Flux Change (%)	Success Rate (%)
Drug X (Allopurinol)	3.5	−20	−10	85
Enzyme Inhibition (Xanthine Oxidase)	4.2	−30	−12	90
Lifestyle Change (Diet/Exercise)	2.0	−10	−5	70

Figures 2a–c presented the metabolic pathway simulations under the influence of allopurinol dosing. Panel (a) illustrates the intravenous plasma & intrahepatic attentiveness shapes for allopurinol and oxypurinol after the multiple doses, indicative of their distribution and metabolism. Panel (b) demonstrates the comparable activity level of the xanthine oxidase (XO) following allopurinol therapy. Panel (c) imitates the intravenous serum and intrahepatic volume profiles of uric acid; thereby demonstrating this drug reduces the concentration of uric acid. These results contribute toward optimizing the treatment of metabolic networks for hyperuricemia.

(a)

(b)

(c)
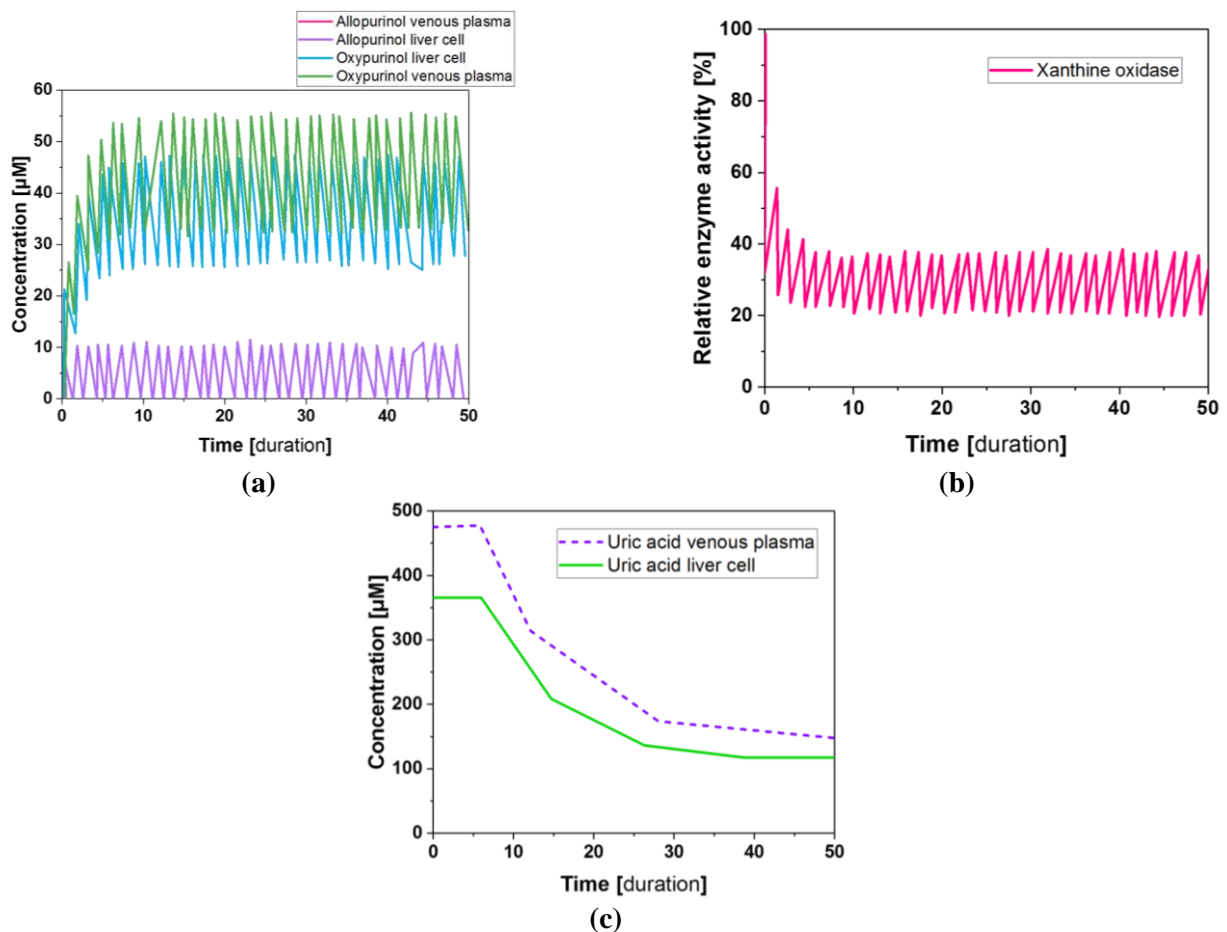
Figure 2. (a) Intravenous plasma & intrahepatic attentiveness shapes for allopurinol and oxypurinol; **(b)** Comparable activity level of the xanthine oxidase (XO); **(c)** Intravenous serum and intrahepatic volume profiles of uric acid.

Figure 3 shows the effects of a urea cycle abnormality and hepatic efflux on metabolic pathways. **Figure 3a** Displays the ammonia concentration patterns in venous plasma and intrahepatic tissues, demonstrating disturbances in detoxification.

Figure 3b Depicts the hepatic efflux levels of urea, alanine, glutamine, & creatinine, which indicate changes in metabolic activity. This helps to optimize cellular metabolic pathways for therapeutic options.

(a)

(b)
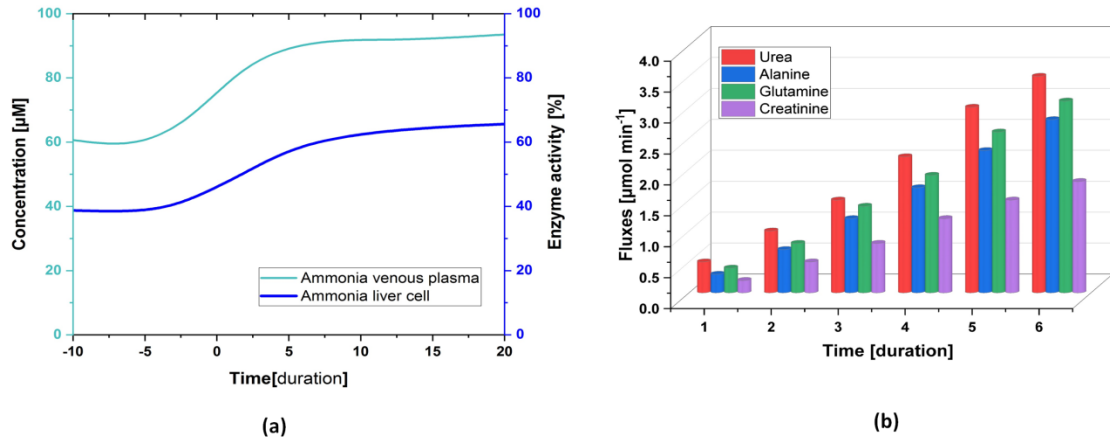
Figure 3. Urea cycle disorder effects on ammonia levels and metabolism.

Figure 4 shows the paracetamol doses at three instances of time affecting liver functionality. **Figure 4a** 1g–5g, **Figure 4b** 6g–10g, and **Figure 4c** 11g–15g doses show a cumulative effect on decreasing the optimal value of objective functions to be considered as the key indicator for liver malfunctioning with an increase in dosage. Simulations for optimizations of metabolic networks prove well for designing strategies concerning safe treatment of liver detoxification with promising metabolic health.

(a)

(b)

(c)
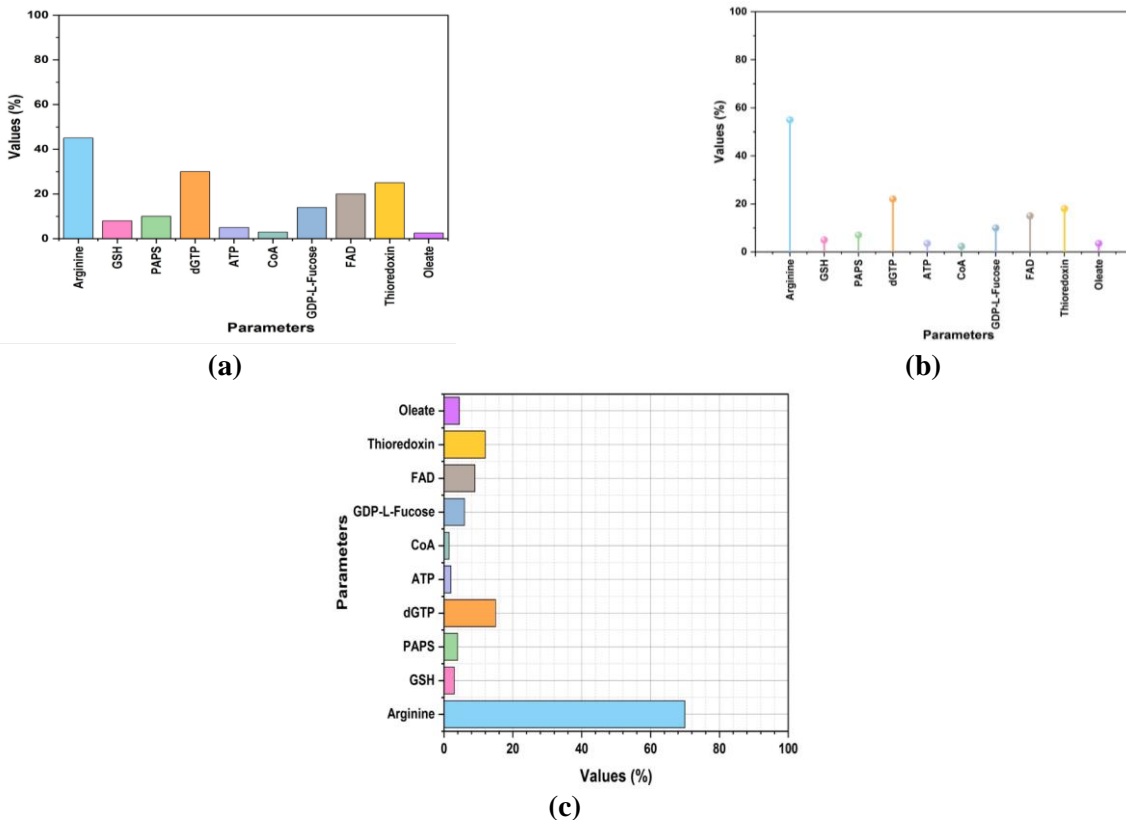
Figure 4. (a) 1g–5g; **(b)** 6g–10g; **(c)** 11g–15g.

5. Discussion and limitations

During the detailed simulation of intricate linkages between cellular metabolic processes and whole-body physiological systems proved to be extremely difficult. There are challenging aspects in metabolic pathways, enzyme kinetics, and dynamic considerations in combination with the integrated application of flux balance analysis with improved genetic algorithms. The findings suggest that baseline doses of treatment cause the decrease of uric acid level from a high of 7.0 mg/d with liver detoxification at 100% and metabolic function at 0%. Therapeutic treatment resulted in a lowered uric acid level of 5.5 mg/dL at the midpoint and 4.0 mg./dL at the endpoint. Liver detoxification increased to 115% at the midpoint and 125% at the end point while Metabolic function improved to moderate to 15% at the midpoint and 25% at the end point. On the other hand, trace doses raised UA to mid and end-point levels of 8.5 and 10.0 mg/dL respectively. Liver detoxification was reduced to 90% at the mid-time point and 75% end time point and metabolic function was reduced to −10% at the mid-time point and −25% end time point imputing a significant liver performance deficit. For 1g–5g (Therapeutic) dose, at the midpoint, glucose metabolism flux is 95%, amino acid metabolism flux 98%, fatty acid metabolism flux 90%, and detoxification flux 97%. At the end-point, the percentage of glucose metabolism flux was augmented to 98 %; amino acid metabolism flux, 99%; fatty acid metabolism flux 98% and detoxification, 99%. At the midpoint of the 6g–10g (Therapeutic) dose, glucose metabolism flux improved by 85%, amino acid by 92%, and fatty acid by 80%, while detoxification by 90%. At the end-point, glucose metabolism flux enhanced to 88% flux, amino acid metabolism flux to 94% flux, fatty acid metabolism flux to 85% flux, and detoxification flux to 92% flux. In the case of 11g–15g (Toxic) dose at the mid-point, the glucose metabolism flux indicated 40%, the amino acid metabolism flux was 50%, the fatty acid metabolism flux was 30% and the detoxification flux was 60%. Finally, the glucose metabolism flux was 25% lower than the baseline, the amino acid metabolism flux, 30% lower than the baseline, the fatty acid metabolism flux 20% lower, and the detoxification flux 40% lower. For Drug X (Allopurinol), the change: the uric acid level was decreased by 3.5 mg/dL the enzyme activity was decreased by 20%, for the metabolic flux 10% was decreased and the success rate was 85%. For example, for Enzyme Inhibition (Xanthine Oxidase), uric acid was lowered by 4.2 mg/dL enzyme activity was lowered by 30% the metabolic flux was lowered to 12% and the success rate was 90%. Likewise for Lifestyle Change (Diet/Exercise), uric acid was lowered by 2.0 mg/dL for the enzyme activity was lowered by 10% The model has drawbacks: it was also limited in explaining individual metabolism differences so could not guarantee consistent results across the patients. Further, the precision of the model may not fully reflect various metabolic aspects of patients due to the use of a simple data set. The fact that the model is based on perfect conditions means that it cannot capture real-life occurrences such as drug interferences or even the long-term effects of a certain drug on the body. In addition, it cannot model the temporal fluctuation in enzyme kinetics and metabolic conversion besides overmedication of drugs. Possibly, the accumulation of larger and more heterogeneous data, as well as the enhancements in the terminology and methodology, including the individual

patient data, or more refined simulations, could be required to improve the model's performance and its usability from the clinical perspective.

6. Conclusion

The conclusion of the research by integrating cellular metabolic processes with whole-body physiological systems, the multi-scale mathematical model could optimize cellular metabolic networks. The model, applying RGA and dynamic flux balance analysis, was able to optimize the activity of enzymes and fluxes of metabolites; hence, it furnished a complex structure for explaining complex biological processes. At therapeutic doses, flux values for glucose, amino acids, fatty acids, and detoxification reached 98%–99%, while toxic doses reduced these to 25%–40%. Treatment strategies were also compared: Allopurinol (3.5 mg/dL uric acid reduction) showed an 85% success rate, enzyme inhibition (4.2 mg/dL reduction) achieved 90%, and lifestyle changes (2.0 mg/dL reduction) had a 70% success rate, demonstrating the model's efficacy in optimizing treatment outcomes. The possibility of applying a treatment model to hyperuricemia brings metabolism in the liver and detoxification pathways as promising areas in drug discovery and treatment strategies for diseases with deeper implications in the field of metabolic optimization, hence offering useful insights for clinical and pharmacological approaches. Future research could spread the model to simulate other metabolic disorders, incorporate personalized medicine approaches, and optimize treatments for various patient profiles.

Author contributions: Conceptualization, HW and YW; writing—original draft preparation, HW and YW; writing—review and editing, HW and YW. All authors have read and agreed to the published version of the manuscript.

Ethical approval: Not applicable.

Conflict of interest: The authors declare no conflict of interest.

References

1. Passi, A., Tibocha-Bonilla, J.D., Kumar, M., Tec-Campos, D., Zengler, K. and Zuniga, C., 2021. Genome-scale metabolic modeling enables an in-depth understanding of big data. Metabolites, 12(1), p.14.https://doi.org/10.3390/metabo12010014
2. Liu, P., Li, Y., Mao, B., Chen, M., Huang, Z. and Wang, Q., 2021. Experimental study on thermal runaway and fire behaviors of large format lithium iron phosphate battery. Applied Thermal Engineering, 192, p.116949. https://doi.org/10.1016/j.applthermaleng.2021.116949
3. Guimarães, C.F., Marques, A.P. and Reis, R.L., 2022. Pushing the natural frontier: Progress on the integration of biomaterial cues toward combinatorial fabrication and tissue engineering. Advanced Materials, 34(33), p.2105645.https://doi.org/10.1002/adma.202105645
4. Schroeder, W.L., Suthers, P.F., Willis, T.C., Mooney, E.J. and Maranas, C.D., 2024. Current State, Challenges, and Opportunities in Genome-Scale Resource Allocation Models: A Mathematical Perspective. Metabolites, 14(7), p.365.https://doi.org/10.3390/metabo14070365
5. Liu, Y., Su, A., Li, J., Ledesma-Amaro, R., Xu, P., Du, G. and Liu, L., 2020. Towards next-generation model microorganism chassis for biomanufacturing. Applied Microbiology and Biotechnology, 104, pp.9095-9108.https://doi.org/10.1007/s00253-020-10902-7
6. Sahu, A., Blätke, M.A., Szymański, J.J. and Töpfer, N., 2021. Advances in flux balance analysis by integrating machine learning and mechanism-based models. Computational and structural biotechnology journal, 19, pp.4626-4640.https://doi.org/10.1016/j.csbj.2021.08.004

7. Sen, P. and Orešič, M., 2023. Integrating Omics Data in Genome-Scale Metabolic Modeling: A Methodological Perspective for Precision Medicine. Metabolites, 13(7), p.855.https://doi.org/10.3390/metabo13070855

8. Tolani, P., Gupta, S., Yadav, K., Aggarwal, S. and Yadav, A.K., 2021. Big data, integrative omics and network biology. Advances in protein chemistry and structural biology, 127, pp.127-160. https://doi.org/10.1016/bs.apcsb.2021.03.006

9. Bernstein, D.B., Sulheim, S., Almaas, E. and Segrè, D., 2021. Addressing uncertainty in genome-scale metabolic model reconstruction and analysis. Genome Biology, 22, pp.1-22. https://doi.org/10.1186/s13059-021-02289-z

10. Miehe, R., Bauernhansl, T., Beckett, M., Brecher, C., Demmer, A., Drossel, W.G., Elfert, P., Full, J., Hellmich, A., Hinxlage, J. and Horbelt, J., 2020. The biological transformation of industrial manufacturing–Technologies, status and scenarios for a sustainable future of the German manufacturing industry. Journal of Manufacturing Systems, 54, pp.50-61. https://doi.org/10.1016/j.jmsy.2019.11.006

11. Bai, L., You, Q., Zhang, C., Sun, J., Liu, L., Lu, H. and Chen, Q., 2023. Advances and applications of machine learning and intelligent optimization algorithms in genome-scale metabolic network models. Systems Microbiology and Biomanufacturing, 3(2), pp.193-206. https://doi.org/10.1007/s43393-022-00115-6

12. Bi, X., Liu, Y., Li, J., Du, G., Lv, X. and Liu, L., 2022. Construction of multiscale genome-scale metabolic models: Frameworks and challenges. Biomolecules, 12(5), p.721.https://doi.org/10.3390/biom12050721

13. Gonçalves, I.G. and García-Aznar, J.M., 2023. Hybrid computational models of multicellular tumour growth considering glucose metabolism. Computational and Structural Biotechnology Journal, 21, pp.1262-1271.https://doi.org/10.1016/j.csbj.2023.01.044

14. Hartmann, F.S., Udugama, I.A., Seibold, G.M., Sugiyama, H. and Gernaey, K.V., 2022. Digital models in biotechnology: towards multi-scale integration and implementation. Biotechnology Advances, 60, p.108015.https://doi.org/10.1016/j.biotechadv.2022.108015

15. Lu, H., Xiao, L., Liao, W., Yan, X. and Nielsen, J., 2024. Cell factory design with advanced metabolic modelling empowered by artificial intelligence. Metabolic Engineering.https://doi.org/10.1016/j.ymben.2024.07.003

16. Gong, Z., Chen, J., Jiao, X., Gong, H., Pan, D., Liu, L., Zhang, Y. and Tan, T., 2024. Genome-scale metabolic network models for industrial microorganism's metabolic engineering: current advances and future prospects. Biotechnology Advances, 72, p.108319.https://doi.org/10.1016/j.biotechadv.2024.108319

17. Ye, C., Wei, X., Shi, T., Sun, X., Xu, N., Gao, C. and Zou, W., 2022. Genome-scale metabolic network models: From first-generation to next-generation. Applied microbiology and biotechnology, 106(13), pp.4907-4920.https://doi.org/10.1007/s00253-022-12066-y

18. Yang, C., Xue, B., Zhang, Y., Wang, S. and Su, H., 2023. Metabolic flux simulation of microbial systems based on optimal planning algorithms. Green Chemical Engineering, 4(2), pp.146-159.https://doi.org/10.1016/j.gce.2022.04.003

19. Wang, X., Mohsin, A., Sun, Y., Li, C., Zhuang, Y. and Wang, G., 2023. From Spatial-Temporal Multiscale Modeling to Application: Bridging the Valley of Death in Industrial Biotechnology. Bioengineering, 10(6), p.744.https://doi.org/10.3390/bioengineering10060744

20. Du, H., Li, M. and Liu, Y., 2023. Towards applications of genome-scale metabolic model-based approaches in designing synthetic microbial communities. Quantitative Biology, 11(1), pp.15-30. https://doi.org/10.15302/J-QB-022-0313

21. Wu, S., Qu, Z., Chen, D., Wu, H., Caiyin, Q. and Qiao, J., 2024. Deciphering and designing microbial communities by genome-scale metabolic modelling. Computational and Structural Biotechnology Journal.https://doi.org/10.1016/j.csbj.2024.04.055

22. Montagud, A., Ponce-de-Leon, M. and Valencia, A., 2021. Systems biology at the giga-scale: Large multiscale models of complex, heterogeneous multicellular systems. Current Opinion in Systems Biology, 28, p.100385.https://doi.org/10.1016/j.coisb.2021.100385

23. Kundu, P., Beura, S., Mondal, S., Das, A.K. and Ghosh, A., 2024. Machine learning for the advancement of genome-scale metabolic modeling. Biotechnology Advances, p.108400.https://doi.org/10.1016/j.biotechadv.2024.108400

24. Nikmaneshi, M.R. and Firoozabadi, B., 2022. Investigation of cancer response to chemotherapy: a hybrid multi-scale mathematical and computational model of the tumor microenvironment. Biomechanics and Modeling in Mechanobiology, 21(4), pp.1233-1249.https://doi.org/10.1007/s10237-022-01587-0

25. Cao, Z., Yu, J., Wang, W., Lu, H., Xia, X., Xu, H., Yang, X., Bao, L., Zhang, Q., Wang, H. and Zhang, S., 2020. Multi-scale data-driven engineering for biosynthetic titer improvement. Current Opinion in Biotechnology, 65, pp.205-212.https://doi.org/10.1016/j.copbio.2020.04.002